Langmuir

Letter

pubs.acs.org/Langmuir

Magnetically Mediated Vortexlike Assembly of Gold Nanoshells

Jianfei Sun,*[,†] Jian Dong,[‡] Dongke Sun,[§] Zhirui Guo,[∥] and Ning Gu*[,†]

[†]State Key Laboratory of Bioelectronics and Jiangsu Key Laboratory of Biomaterials and Devices, School of Biological Science and Medical Engineering, Southeast University, Nanjing 210009, P. R. China

[‡]State Key Laboratory of Bioelectronics, School of Biological Science and Medical Engineering, Southeast University, Nanjing 210096, P. R. China

[§]School of Mechanic Engineering, Southeast University, Nanjing 210096, P. R. China

[∥]The Second Affiliated Hospital of Nanjing Medical University, Nanjing 210011, P. R. China

Supporting Information

ABSTRACT: Gold nanoshells currently attract increasing research interests due to the important role in many subjects. For practical applications, random arrangement of the nanoparticles is often unfavored so that the assembly of gold nanoshells is becoming a central issue. We here proposed to utilize time-variant magnetic field to direct the assembly of gold nanoshells. It was discovered that the alternating magnetic field can mediate the vortex-like assembly of gold nanoshells. The mechanism was explored and thought to be relative with the electric field of induction which caused the thermal gradient on the substrate and the electric force. The vortexlike structure as well as the assembly mechanism will play an important role in research and application of gold nanomaterials.

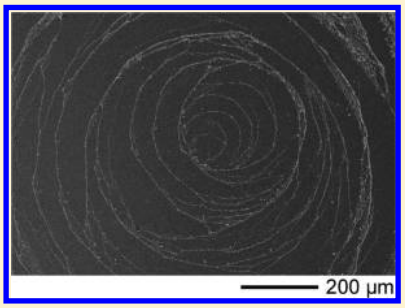

INTRODUCTION

Thanks to the pioneering work of Halas and West,[1] gold nanoshells currently attract increasing research interests due to the important role in many subjects such as plasmonics,[2] photothermal therapy,[3] and SERS (surface enhanced raman spectrum)-based dection.[4] For research of plasmonics, the relationship between arrangement of unit blocks and distribution of light is a key issue. Availability of novel structures of nanomaterials will obviously contribute to the research. This is likewise the case for the photothermal therapy. As a heating source, different aggregation of the gold nanoshells will lead to the different thermal transfer and distribution which is closely correlative with the therapeutic performance. For the SERS-based sensing, the arrangement of nanomaterials on substrate should be uniform and recognizable so that the signals can be gathered correctly. If the nanoparticles are randomly arranged, the detection will be irreproducible. Moreover, the assembled pattern will contribute to the fundamental research on interaction between the nanoparticles and the cells. We have discovered that the arrangement of nanoparticles on the substrate can direct and regulate the growth of osteoblasts. However, the phenomena disappeared when the nanoparticles were randomly arranged. The novel structures of nanoparticulate assemblies will certainly play an important role in the elucidation of this phenomenon.

Magnetic field-directed self-assembly has advantages of low cost, good reproducibility, large scale, and unnecessity of extra molecules.[5] The static magnetic field has been employed to direct the assembly of magnetic nanomaterials, resulting in formation of the one-dimensional chains with microstructures.[6,7] Although the magnetically directed assembly seems adoptive for arrangement of the gold nanoshells, the gold nanoshells are incapable of being directly manipulated by the static magnetic field due to the weak susceptibility. However, time-variant magnetic field is considered to be able to assemble the gold nanoshells based on our previous observations that the time-variant magnetic field can induce both magnetic nanoparticles and gold nanoparticles to form the special patterns.[8−10] The manipulation of weakly magnetic objects by the time-variant magnetic field is mainly dependent upon the effects of electromagnetic induction, which are variable in specific cases. Thus, the study of gold nanoshell assembly in the presence of the time-variant magnetic field is an important and interesting issue. In this Letter, it is reported that the gold nanoshells can form vortexlike assemblies mediated by the alternating magnetic field and the mechanism may lie in the complex effect of the electric field of induction.

EXPERIMENTAL SECTION

The gold nanoshells, stabilized by citric acid, were synthesized by following Halas' method without removing the SiO_2 cores.[11] As seen from TEM image of the synthesized nanoshells (see Figure 1A), the size of the particles was estimated to approximate 160 nm. All the chemical reagents during the process of synthesis were dissolved in the pure water, and the final colloidal suspension was also aqueous phased. The concentration of the gold nanoshells in the experiments was 33.4 μg/mL, measured by using an atomic absorption spectrometer. The strength of the alternating magnetic field in our experiments was fixed on 70 KA/m, and the frequency ranged from 20 Hz to 100 kHz.

Received: January 15, 2012
Revised: March 30, 2012
Published: April 2, 2012

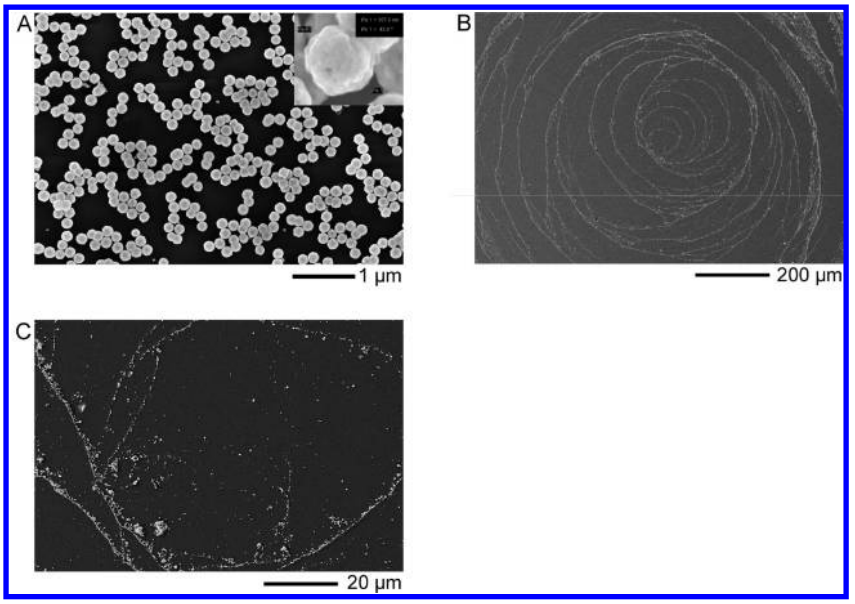

Figure 1. Gold nanoshells for assembly. (A) SEM image of the synthesized gold nanoshells. Inset: size measurement of one particle. (B) SEM image of the gold nanoshells after field-mediated assembly. (C) Local magnification of central area of (B).

Si wafer was used as substrate for supporting the colloidal droplet. The substrates in the experiments, including Si wafers and glass cover slides, were cleaned by using a mixture of H_2SO_4 and H_2O_2 at the boiling temperature. The flux of magnetic field was always perpendicular to the Si wafer as described in our previous reports.[8,9] The motion of particles in the presence of field was simulated with the Lattice-Boltzmann method.

RESULTS AND DISCUSSION

Generally speaking, the colloidal particles form the amorphous aggregates after the solvent evaporation. However, the nanoshells assembled into the vortexlike pattern in the presence of 100 kHz alternating magnetic field (see Figure 1B and C). However, the phenomenon was incapable of occurring either under the fields below 100 kHz or on glass substrates. Instead, the gold nanoshells formed the small aggregates discretely dispersing on the substrate (see Supporting Information, Figure S1). Here it should be mentioned that the pattern formation was not merely dependent upon the field frequency. In our experiments, an alternating magnetic field that owned the fixed frequency (40 kHz) but the adjustable intensity was also employed to assemble the gold nanoshells. The results indicated that the gold nanoshells can also form the vortex-like pattern of the kind when the field intensity was above 110 KA/m. However, the gold nanoshells failed to form such a pattern on the glass substrate even under the higher field intensity.

Because the gold nanoshell is weakly magnetic substance, the electric field of induction was taken into account. According to Faraday's rule of the electromagnetic induction, an alternating magnetic field will generate an electric field with identical frequency ($\nabla \times \vec{E} = (\partial\vec{B}/\partial t)$). In our experiments, the induction field was a circular electric field in the plane of substrate. Our Si wafers were commercially available, and the impedance was measured to be 2 KΩ (Supporting Information, Figure S2). Hence, the electric field of induction is to result in more thermal production of the Si wafer with the frequency of alternating magnetic field increasing. Actually, the colloidal droplet was observed to evaporate much more quickly under the treatment of the 100 kHz alternating magnetic field. In experiments, the steam was observed to emerge after 1 min treatment of the 100 kHz alternating magnetic field. After 4 min, the droplet began to shrink and dried thoroughly in one more minute.

The heating curve of a Si wafer (there is a drop of solution on it) under the treatment of 100 kHz alternating magnetic field is shown in Figure 2A, exhibiting that temperature of the Si wafer increased swiftly to approximate 80 °C in 1 min and this temperature was kept for 4 min. After that, the temperature increased sharply again, meaning the solution had evaporated thoroughly. Associated with the experimental phenomena, it was inferred that the assembly was ongoing in the stage of 80 °C. For this reason, the surface thermal distribution of Si wafer was simulated, which showed a concentrically ringed pattern (see Figure 2B). A heating platform was likewise adjusted to 80 °C in order to inspect the influence of the thermal gradient in the absence of the alternating magnetic field. The after-dried pattern is shown in Figure 2C (the corresponding local magnification is shown in Figure 2D), which is somewhat similar to that of the simulation. Here, the aggregation of nanoparticles was considered to be driven by the gradient of thermal energy ($F = -\nabla U$, where F is force and U is energy). In Figure 2B, the color denoted temperature and the maximal variety of thermal energy are present in the regions of color transition. Therefore, the nanoparticles tended to aggregate into the concentrically ringed pattern.

Besides inducing the thermal gradient, the electric field of induction also imposed force on the gold nanoshells. Movements of one particle and two particles in the presence of the circular electric field were simulated with neglecting the influence of Brownian motion, respectively. Both animations can be seen in the Supporting Information (movies S1 and S2). The moving trajectory of one particle is shown in Figure 3A, demonstrating that the particle may make a spiral motion under the circular electric field. For two particles, the simulation demonstrated that the back one can move more quickly than the front one, which can account for the linkage between the interior rings and the exterior rings. The electric force here includes the electrostatic force and the dielectrophoretic force because the induction field is alternating electric field. The former

dx.doi.org/10.1021/la300212d | Langmuir 2012, 28, 6520−6526

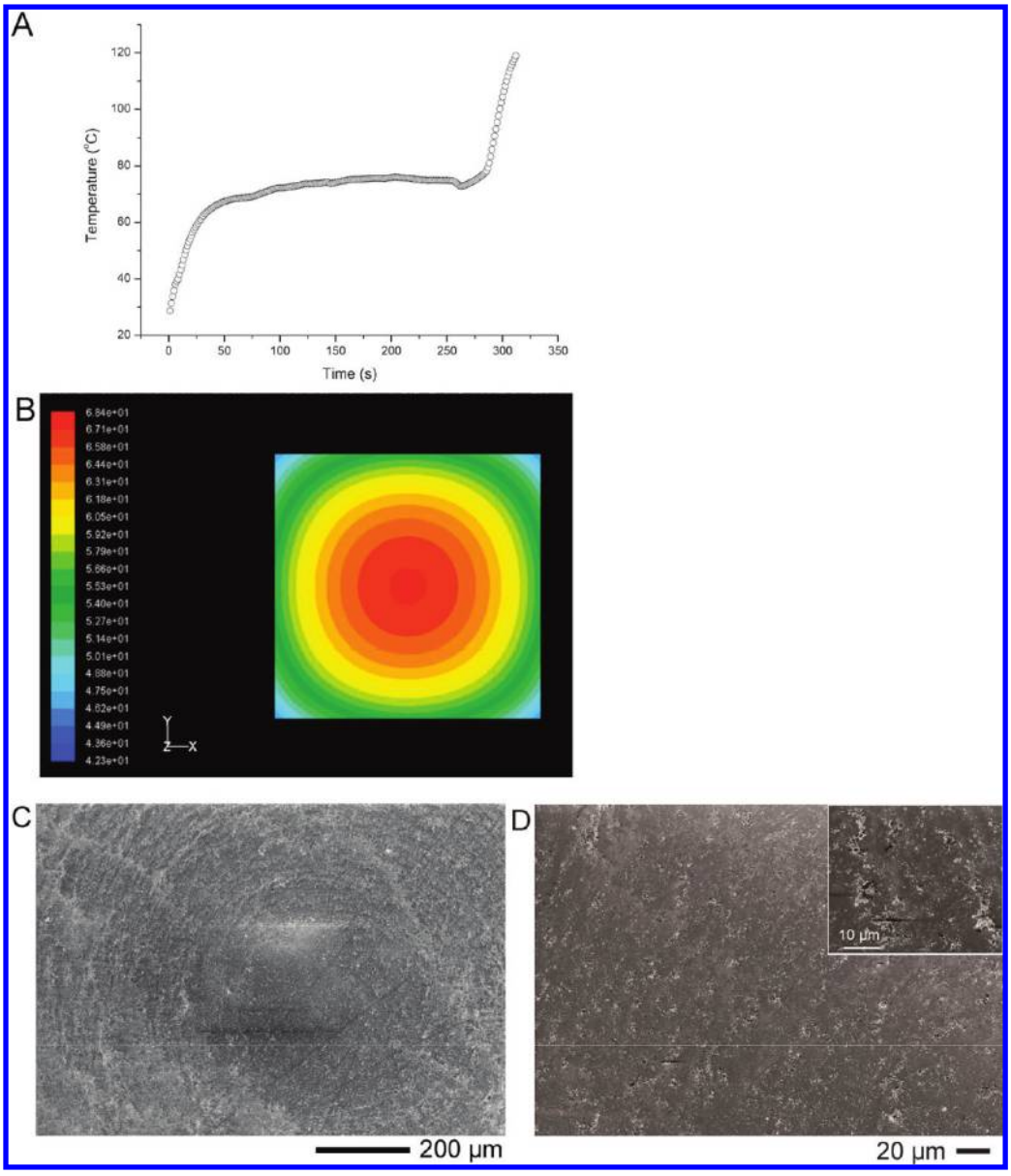

Figure 2. Influence of thermal distriution of Si substrate on assembly of gold nanoshells. (A) Temperature measurement of Si wafer during process of the assembly. (B) Simulation of thermal gradient on Si surface after 4 minutes. (C) SEM image of gold nanoshells after drying on an 80 °C heating stage in the absence of alternating magnetic field. (D) Local magnification of (C). Inset: local magnification of (D).

arises from the Coulomb interaction, dependent upon the net charges of particles. The force can be expressed by

$$\vec{F}_{EP} = q \cdot \vec{E} \quad (1)$$

where $\vec{F}_{EP}$ is the electrostatic force, q is the net charges of objects, and $\vec{E}$ is the intensity of electric field. According to the reaction mechanism of gold nanoshells synthesis, there were amounts of citric radicals adsorbed on the surface of gold nanoshells so that the gold nanoshells are charged, capable of being driven by the electrostatic force. The latter arises from the polarization of objects under the alternating electric field, dependent upon the size and the polarizability rather than the net charges. This force is often called dielectrophoretic, expressed by

$$\vec{F}_{DEP} = 2\pi\varepsilon r^3 \mathrm{Re}[K(\omega)]\nabla|\vec{E}|^2 \quad (2)$$

where $\vec{F}_{DEP}$ is the dielectrophoretic force, ε is the complex permittivity, r is the radius of object, $\mathrm{Re}[K(\omega)]$ is the Clausius-Mossotti factor that is derived from the effective polarizability. and $\vec{E}$ is the intensity of electric field.[12]

Based on the above-mentioned analysis, a possible mechanism of assembly was schematically depicted in Figure 3B, which relied on the synergetic effect of electric force and substrate heating. The first step was that the nanoshells formed the loosely packed aggregates resulting from the thermal gradient, which is similar to the concentrically ringed pattern. After that the nanoshells were directed to move spirally, further to form the close-packed vortexlike assemblies. During the process, the directed spiral motion in the second stage was activated just on the basis of the aggregation of gold nanoshells in the first stage. Seen from eqs 1 and 2, the aggregation of building units enlarges the total charge and volume of the objects so that the electric force gets enhanced to be capable of overcoming the thermal and fluidic resistance. That is why

dx.doi.org/10.1021/la300212d | *Langmuir* 2012, 28, 6520−6526

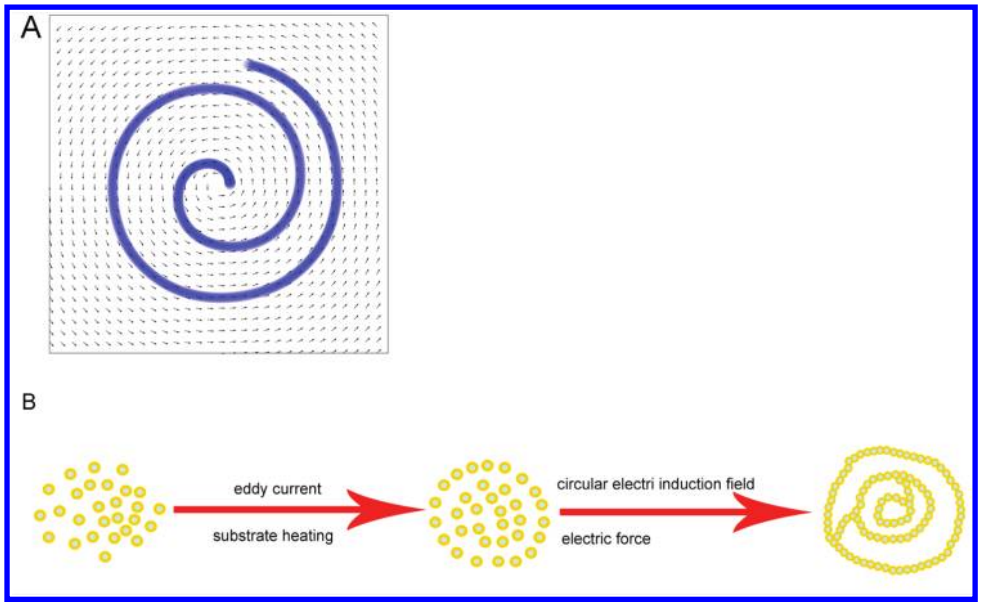

Figure 3. Mechanism of vortexlike assembly. (A) Simulated trajectory of one particulate movement driven by circular electric field. (B) Schematic depiction of the pattern formation of gold nanoshells.

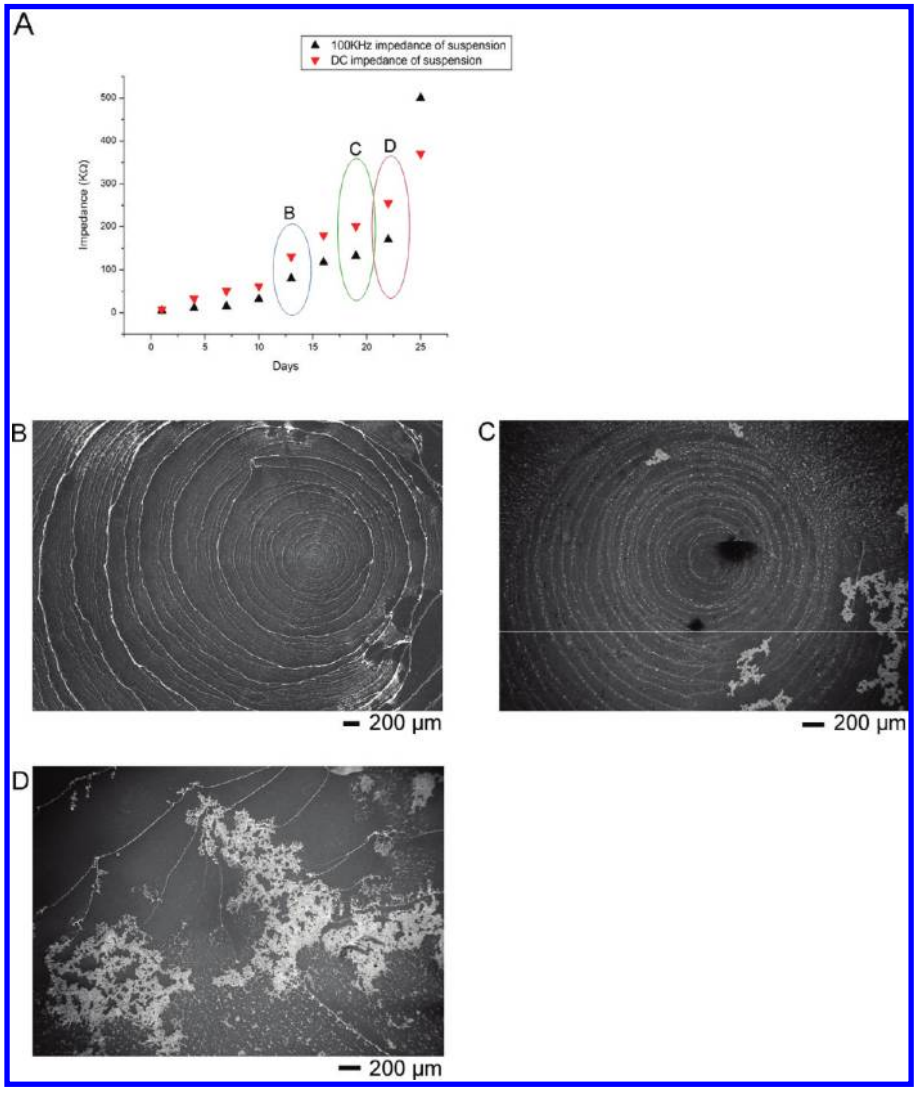

Figure 4. SEM images of nanoshells assembly with ion amount decreasing. (A) Impedance of the colloidal suspension versus the time. (B–D) Typical SEM images of particulate assemblies in three time points.

dx.doi.org/10.1021/la300212d | *Langmuir* 2012, 28, 6520–6526

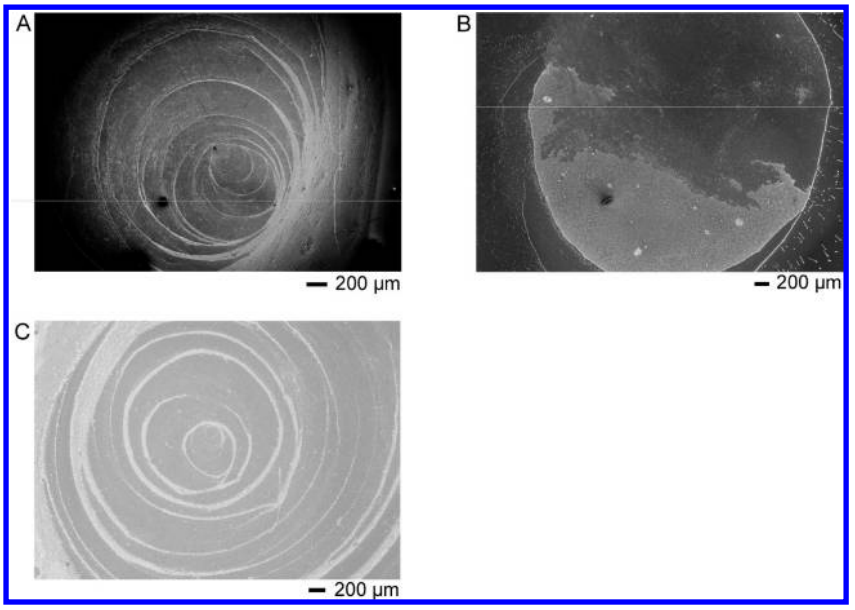

Figure 5. Field-mediated assembly of 40 nm hollow Au nanoshells and 10 nm Au nanoparticles. (A) SEM image of 40 nm gold nanoshells after 100 kHz alternating magnetic field-mediated assembly. (B) SEM image of 10 nm gold nanoparticles after 100 kHz alternating magnetic field-mediated assembly. (C) SEM image of 10 nm colloidal gold aggregates after 100 kHz alternating magnetic field-mediated assembly.

neither the thermal gradient nor the electric field of induction can lead to the pattern formation solely.

The dependence of the pattern formation upon the colloidal ion amount was also experimentally studied. The suspension of nanoshells was settled for 3 days until the lamination can be observed. Then the supernatant was removed and the ultrapure water (resistivity $\geq$ 18.25 MΩ·cm^{-1}) of the same volume was added into the suspension. By repeating this process, the ion amount can be incessantly decreased. The ion amount of the colloidal system was characterized by measuring impedance of the suspension. The data are plotted in Figure 4A (the ion amount decreased every 3 days, and hence the number of days was used as the abscissa). It was experimentally discovered that there was a transition from the vortexlike pattern into the concentric-circled pattern with the ion amount decreasing (see Figure 4B and C). Furthermore, the assembled structure vanished when the ion amount was too small (see Figure 4D). The measurements of ζ potential as well as DLS (dynamic light scattering) confirmed that the surface charges of nanoshells were reduced with colloidal ions becoming less and less, and the nanoshells were inclined to form the larger aggregates (Supporting Information, Figure S3). According to eqs 1 and 2, the electrostatic force becomes smaller while the dielectrophoretic force becomes larger. Therefore, the assembled pattern can be controlled by the synergetic action of the two electric forces, the thermal gradient and the Brownian and fluidic resistance. When the electric force was too weak to overcome the resistance, the influence from the thermal gradient of substrate was to play a dominant role so that the gold nanoshells formed the concentric circles. However, when the charges were too few to stabilize the colloidal particles, the nanoshells promptly formed the amorphous aggregates to achieve the thermal equilibrium.

Then 40 nm hollow Au nanoshells[13,14] and 10 nm Au nanoparticles were also employed as the building blocks for the field-mediated assembly. Both the nanomaterials were stabilized by the citric acid. The SEM image of as-synthesized 40 nm hollow gold nanoshells is shown in the Supporting Information (Figure S4). The morphological images of both the nanoparticles after field-mediated assembly are shown in Figure 5A and B. For the 40 nm hollow nanoshells, the vortexlike assembly can also occur but the assemblies were much more loosely packed and dispersive. However, the assembly failed to take place for the 10 nm gold nanoparticles. Interestingly, if the 10 nm colloidal gold particles aggregated into the larger clusters,[15] the vortexlike assembly was to reappear (see Figure 5C). The mean size and the ζ potential of the aggregated clusters were measured to be 164 nm and −23.74 mV, respectively (Supporting Information, Figure S5), revealing that this phenomenon resulted from the enhancement of the electric force due to the enlargement of building blocks so that the Brownian motion and the fluidic resistance can be overcame.

The entropy-driven effect is possible to result in the formation of ringlike patterns. The influence of this factor was excluded by probing the relationship between the pattern formation and the concentration of gold nanoshells after natural drying. We set six concentrations, and the conformational images after natural drying are shown in the Supporting Information (Figure S6). The after-dried conformation of gold nanoshells was randomly dispersive, and there was little difference among the samples. Therefore, our experimental phenomena are not caused by the entropy-driven effect. The experiments of different concentration can also partly exclude the "coffee ring" effect, which roots in the pinning of the contact line of colloidal droplet. Because the dilution was done by adding the ultrapure water, the gold nanoshells turned more and more unstable. However, the "coffee ring" structure failed to emerge for all the samples. This result means that the formation of the vortexlike structure is different from that of the "coffee ring" structure in mechanism. It was recently reported that the anisotropic particles can suppress the "coffee ring" effect.[16] We furthermore verified that the time-variant magnetic field-mediated vortexlike assembly was independent upon the contact line of colloidal droplet. The CTAB-capped gold nanorods (40 nm, aspect ratio is 3) were employed as the building blocks for the time-variant magnetic field-mediated assembly. Unlike the suppression of

dx.doi.org/10.1021/la300212d | *Langmuir* 2012, 28, 6520−6526

the formation of "coffee ring", the time-variant magnetic field can also induce the vortexlike assembly of the gold nanorods (Supporting Information, Figure S7). Thus, the vortexlike assembly of the gold nanoshells should be a novel phenomenon of pattern formation which is mediated by the field.

Here, it should be mentioned that the assembly time may be important for the pattern formation. However, the characterization of the assembly process in situ becomes very difficult because any conducting material will be molten due to the presence of the powerful alternating magnetic field. We previously probed the influence of different assembly time on the pattern formation of magnetic nanoparticles. The assembly time for the magnetic nanoparticles was much longer than that for the gold nanoshells. The minimal available time for assembly was 9 min and the maximal available time for assembly was 4 h. The results revealed that the nanoparticles formed the amorphous clusters randomly dispersing on the substrate for the minimal assembly time. With the assembly time prolonged, the assembled patterns turned more and more ordered. Thus, we inferred that the nanoparticles first formed the clusters and after that the clusters further were rearranged to form the ordered patterns under the treatment of external field.

CONCLUSION

In conclusion, it is discovered that the time-variant magnetic field can mediate the vortexlike assembly of gold nanoshells. The mechanism lies in the electric field of induction which gives rise to the thermal gradient and the electric force to synergistically assemble the gold nanoshells into the vortexlike pattern. This report will deepen the knowledge of the field-directed assembly and widen the application of gold nanomaterials. In addition, the alternating magnetic field will attract more attentions for the directed assembly of weak magnetic objects.

ASSOCIATED CONTENT

Supporting Information

Morphological images of gold nanoshells after assembly, impedance measurement of Si wafer as the substrate, measurements of DLS and ζ potential for nanoshells with ion amount decreasing, SEM image of 40 nm hollow Au nanoshells, mean size and ζ potential of 10 nm Au nanoparticulate aggregates, the morphological images of gold nanoshells with different concentrations after natural drying, the pattern formation of gold nanorods mediated by the alternating magnetic field. This material is available free of charge via the Internet at http://pubs.acs.org.

AUTHOR INFORMATION

Corresponding Author

*E-mail: guning@seu.edu.cn (N.G.); sunzaghi@seu.edu.cn (J.S.).

Notes

The authors declare no competing financial interest.

ACKNOWLEDGMENTS

This work is supported by grants from the National Natural Science Foundation of China (NSFC, 20903021, 81100625), the National Basic Research Program of China (2011CB933503) and the US-China international S & T cooperation project (2009DFA31990). J. Sun is also thankful to the supports from the Research Fund for the Doctoral Program of Higher Education of China (20090092120036), the Natural Science Foundation of Jiangsu Province (BK2011590) and the special fund for the top doctoral thesis of Chinese Education Ministry. Dr. Ruizhi Xu, Miss Lei He and Miss Bei Yao are also greatly appreciated for their works in the previous experiments.

REFERENCES

(1) West, J. L.; Halas, N. J. Engineered Nanomaterials for Biophotonics Applications: Improving Sensing, Imaging, and Therapeutics. *Annu. Rev. Biomed. Eng.* **2003**, *5*, 285−292.

(2) (a) Halas, N. J.; Lal, S.; Chang, W.-S.; Link, S.; Nordlander, P. Plasmons in Strongly Coupled Metallic Nanostructures. *Chem. Rev.* **2011**, *111*, 3913−3961. (b) Zhang, H.; Li, Y.; Ivanov, I. A.; Qu, Y.; Huang, Y.; Duan, X. Plasmonic Modulation of the Upconversion Fluorescence in NaYF:YB/Tm Hexaplate Nanocrystals Using Gold Nanoparticles or Nanoshells. *Angew. Chem., Int. Ed.* **2010**, *49*, 2865−2868. (c) Wang, M.; Cao, M.; Chen, X.; Gu, N. Subradiant Plasmon Modes in Multilayer Metal-Dielectric Nanoshells. *J. Phys. Chem. C* **2011**, *115*, 20920−20925.

(3) (a) Liu, H.; Chen, D.; Li, L.; Liu, T.; Tan, L.; Wu, X.; Tang, F. Multifunctional Gold Nanoshells on Silica Nanorattles: A Platform for the Combination of Photothermal Therapy and Chemotherapy with Low Systemic Toxicity. *Angew. Chem., Int. Ed.* **2011**, *50*, 891−895. (b) Melancon, M. P.; Lu, W.; Yang, Z.; Zhang, R.; Cheng, Z.; Elliot, A. M.; Stafford, J.; Olson, T.; Zhang, J. Z.; Li, C. Therapeutics, Targets, and Development: In vitro and In vivo Targeting of Hollow Gold Nanoshells Directed at Epidermal Growth Factor Receptor for Photothermal Ablation Therapy. *Mol. Cancer Ther.* **2008**, *7*, 1730−1739. (c) Lal, S.; Clare, S. E.; Halas, N. J. Nanoshell-Enabled Photothermal Cancer Therapy: Impending Clinical Impact. *Acc. Chem. Res.* **2008**, *41*, 1842−1851.

(4) (a) Kšitner, B.; Gellner, M.; Schütz, M.; Schöppler, F.; Marx, A.; Ströbel, P.; Adam, P.; Schmuck, C.; Schlücker, S. SERS Labels for Red Laser Excitation: Silica-Encapsulated SAMs on Tunable Gold/Silver Nanoshells. *Angew. Chem., Int. Ed.* **2009**, *48*, 1950−1953. (b) Zhang, Q.; Ge, J. P.; Goebl, J.; Hu, Y. X.; Sun, Y. G.; Yin, Y. D. Tailored Synthesis of Superparamagnetic Gold Nanoshells with Tunable Optical Properties. *Adv. Mater.* **2010**, *22*, 1905−1909. (c) Yang, M.; Alvarez-Puebla, R.; Kim, H.-S.; Aldeanueva-Potel, P.; Liz-Marza, L. M.; Kotov, N. A. SERS-Active Gold Lace Nanoshells with Built-in Hotspots. *Nano Lett.* **2010**, *10*, 4013−4019.

(5) (a) Daniel, M.-C.; Astruc, D. Gold Nanoparticles: Assembly, Supramolecular Chemistry, Quantum-Size-Related Properties, and Applications toward Biology, Catalysis, and Nanotechnology. *Chem. Rev.* **2004**, *104*, 293−346. (b) Sun, J.; Gu, N. Electromagnetic Manipulation of Colloidal Nanoparticles. *Ency. Nanosci. Nanotechnol.* **2011**, *13*, 355−374.

(6) Hu, M. J.; Lin, B.; Yu, S. H. Magnetic Field-Induced Solvothermal Synthesis of One-Dimensional Assemblies of Ni-Co Alloy Microstructures. *Nano Res.* **2008**, *1*, 303−313.

(7) Liu, Y.; Zhou, L.; Hu, Y.; Guo, C.; Qian, H.; Zhang, F.; Lou, X. W. Magnetic-Field Induced Formation of 1D Fe_3O_4/C/CdS Coaxial Nanochains as Highly Efficient and Reusable Photocatalysts for Water Treatment. *J. Mater. Chem* **2011**, *21*, 18359−18364.

(8) Sun, J.; Zhang, Y.; Chen, Z.; Zhou, J.; Gu, N. Fibrous Aggregation of Magnetite Nanoparticles Induced by a Time-Varied Magnetic Field. *Angew. Chem., Int. Ed.* **2007**, *46*, 4767−4770.

(9) Sun, J.; Mao, Y.; Guo, Z.; Zhang, Y.; Gu, N. Alternating-Magnetic-Field Induced Monolayer Formation and Re-aggregation of Au Nanoparticles During Solvent Evaporation. *J. Nanosci. Nanotechnol.* **2009**, *9*, 1156−1159.

(10) Sun, J.; Sui, Y.; Wang, C.; Gu, N. The Investigation of Frequency Response for The Magnetic Nanoparticulate Assembly Induced by Time-varied Magnetic Field. *Nanoscale Res. Lett.* **2011**, *6*, 453−458.

(11) Oldenburg, S. J.; Averitt, R. D.; Westcott, S. L.; Halas, N. J. Nanoengineering of Optical Resonances. *Chem. Phys. Lett.* **1998**, *288*, 243−247.

(12) Minerick, A. R.; Zhou, R.; Takhistov, P.; Chang, H.-C. Manipulation and Characterization of Red Blood Cells with Alternating Current Fields in Microdevices. *Electrophoresis* **2003**, *24*, 3703−3717.
(13) The first Ag nanoparticle colloid was prepared by thermal reduction of 10 mM $AgNO_3$ aqueous solution in the presence of 15 mM trisodium citrate at 90 °C. After the solution had turned green within 30 s, it was cooled quickly in the ice bath. The synthesized colloid (30 mL) was reacted with 6 mL of 1 mM $HAuCl_4$ at boiling conditions to form gold nanoshells through a template-engaged replacement reaction process.
(14) Skrabalak, S. E.; Chen, J.; Sun, Y.; Lu, X.; Au, L.; Cobley, C. M.; Xia, Y. Gold Nanocages: Synthesis, Properties, and Applications. *Acc. Chem. Res.* **2008**, *41*, 1587−1595.
(15) The 10 nm colloidal Au was synthesized by the classic reduction of $HAuCl_4$ with citric acid. The solution showed a red-wine color, meaning the size approximated 10 nm. We added a very tiny amount of salt into the solution. Then the colloidal solution seemed dark gray, meaning the aggregation occurred.
(16) Yunker, P. J.; Still, T.; Lohr, M. A.; Yodh, A. G. Suppression of The Coffee-ring Effect by Shape-dependent Capillary Interactions. *Nature* **2011**, *476*, 308−311.